

# CONSTRAINING THE LIFETIME OF QUASARS FROM THEIR SPATIAL CLUSTERING

ZOLTÁN HAIMAN<sup>1</sup>

Princeton University Observatory, Princeton, NJ 08544, USA  
 email: zoltan@astro.princeton.edu

AND

LAM HUI

Institute for Advanced Study, Olden Lane, Princeton, NJ 08544, USA  
 email: lhui@ias.edu

*ApJ*, in press (submitted on Feb. 8. 2000)

## ABSTRACT

The lifetime of the luminous phase of quasars is constrained by current observations to be  $10^6 \lesssim t_Q \lesssim 10^8$  years, but is otherwise unknown. We model the quasar luminosity function in detail in the optical and X-ray bands using the Press–Schechter formalism, and show that the expected clustering of quasars depends strongly on their assumed lifetime  $t_Q$ . We quantify this dependence, and find that existing measurements of the correlation length of quasars are consistent with the range  $10^6 \lesssim t_Q \lesssim 10^8$ . We then show that future measurements of the power spectrum of quasars out to  $z \sim 3$ , from the 2dF or Sloan Digital Sky Survey, can significantly improve this constraint, and in principle allow a precise determination of  $t_Q$ . We estimate the systematic errors introduced by uncertainties in the modeling of the quasar-halo relationship, as well as by the possible existence of obscured quasars.

*Subject headings:* cosmology: theory – cosmology: observation – quasars: formation – large scale structure

## 1. INTRODUCTION

A long outstanding problem in cosmology is the synchronized evolution of the quasar population over the redshift range  $0 \lesssim z \lesssim 5$ . Observations in the optical (Pei 1995) and radio (Shaver et al. 1994) show a pronounced peak in the abundance of bright quasars at  $z \approx 2.5$ ; recent X-ray observations (Miyaji et al. 2000) confirm the rapid rise from  $z = 0$  towards  $z \approx 2$ , but have not shown evidence for a decline at still higher redshifts. Individual quasars are widely understood to consist of supermassive black holes (BHs) powered by accretion (Lynden-Bell 1967; Rees 1984). A plausible timescale for quasar activity is then the Eddington time,  $4 \times 10^7 (\epsilon/0.1)$  yr, the e-folding time for the growth of a BH accreting mass at a rate  $\dot{M}$ , while shining at the Eddington luminosity with a radiative efficiency of  $L = L_{\text{Edd}} = \epsilon \dot{M} c^2$ . The lifetime  $t_Q$  of the luminous phase of quasars can be estimated directly, by considering the space density of quasars and galaxies. At  $z \sim 2$ , the ratio  $n_Q/n_G \sim 3 \times 10^{-3}$  implies the reassuringly close value of  $t_Q \sim t_{\text{Hubble}} n_Q/n_G \sim 10^7$  yr (Blandford 1999 and references therein). These lifetimes are significantly shorter than the Hubble time, suggesting that the quasar population evolves on cosmic time-scales by some mechanism other than local accretion physics near the BH.

It is tempting to identify quasars with halos condensing in a cold dark matter (CDM) dominated universe, as the halo population naturally evolves on cosmic time-scales (Efsthathiou & Rees 1988; Haiman & Loeb 1998; Kauffmann & Haehnelt 2000). Furthermore, quasars reside in a subset of all galaxies, while the redshift–evolution of the galaxy population as a whole (qualitatively similar to that of bright quasars) has been successfully described by asso-

ciating galaxies with dark halos (e.g. Lacey & Cole 1993; Kauffmann & White 1993). A further link between galaxies and quasars comes from the recent detection, and measurements of the masses of massive BHs at the centers of nearby galaxies (Magorrian et al. 1998; van der Marel 1999).

These arguments suggest that the evolution of the quasar population can indeed be described by “semi-analytic” models, associating quasars with dark matter halos. In this type of modeling, the quasar lifetime plays an important role. The quasar phase in a single halo could last longer ( $t_Q \sim 10^8$  yr), with correspondingly small  $M_{\text{bh}}/M_{\text{halo}}$  ratios, or last shorter ( $t_Q \sim 10^6$  yr), with larger BH formation efficiencies (Haiman & Loeb 1998; Haehnelt et al. 1998). Note that although recent studies have established a correlation between the bulge mass  $M_{\text{bulge}}$  and BH mass  $M_{\text{bh}}$ , this correlation leaves a considerable uncertainty in the relation between  $M_{\text{bh}}$  and the mass  $M_{\text{halo}}$  of its host halo. If the initial density fluctuations are Gaussian with a CDM power spectrum, the clustering of collapsed halos is a function of their mass – rarer, more massive halos cluster more strongly (Kaiser 1984; Mo & White 1996). Hence, measurements of quasar clustering are a potentially useful probe of both BH formation efficiencies and quasar lifetimes (La Franca et al. 1998; Haehnelt et al. 1998).

In this paper, we assess the feasibility of breaking the above degeneracy, and inferring quasar lifetimes, from the statistics of clustering that will be available from the Sloan Digital Sky Survey (SDSS, Gunn & Weinberg 1995) and Anglo-Australian Telescope Two-Degree-Field (2dF, Boyle et al. 1999). Previous works (e.g. Stephens et al. 1997; Sabbey et al. 1999) have yielded estimates suggesting

<sup>1</sup>Hubble Fellow

that quasars are clustered more strongly than galaxies. However, the current uncertainties are large, especially at higher redshifts, where clustering has been found to decrease (Iovino & Shaver 1988; Iovino et al. 1991), to stay constant (Andreani & Cristiani 1992; Croom & Shanks 1996), or to increase with redshift (La Franca et al. 1998). As a result, no strong constraints on the life-time can be obtained yet. The key advance of forthcoming surveys over previous efforts is two-fold. Because of their sheer size, i.e. the large number of quasars covering a large fraction of the sky, both shot-noise and sample variance can be beaten down, significantly reducing the statistical uncertainties. Furthermore, the large sample-size will eliminate the need to combine data from different surveys with different selection criteria, hence allowing cleaner interpretation.

Recent measurements of the local massive black hole density have stimulated discussions of a radiative efficiency which is much lower than the usual  $\sim 0.1$  (e.g. Haehnelt et al. 1999). A convincing constraint on the lifetime of quasars could be therefore highly interesting, as this might have implications for the local accretion physics near the BH.

This paper is organized as follows. In § 2, we summarize our models for the quasar luminosity function, and in § 3 we compute the quasar correlation function in these models. In § 4, we compare the model predictions with presently available data, and in § 5 we assess the ability of future optical redshift surveys to discriminate between the various models. In § 6, we repeat our analysis in the soft X-ray band, and examine the contribution of quasars to the X-ray background, and its auto-correlation. In § 7, we address some of the caveats arising from our assumptions, and in § 8 we summarize our conclusions and the implications of this work.

## 2. MODELS FOR THE QUASAR LUMINOSITY FUNCTION

In this section, we briefly summarize our model for the luminosity function (LF) of quasars, based on associating quasar BHs with dark halos. Our treatment is similar to previous works (Haiman & Loeb 1998; Haehnelt et al. 1998), although differs in some of the details. A more extensive treatment is provided in the Appendix. The main assumption is that there is, on average, a direct monotonic relation between halo mass  $M_{\text{halo}}$  and average quasar luminosity  $L_{M,z}$ , which we parameterize using the simple power-law ansatz:

$$\bar{L}_{M,z} = x_0(z) M_{\text{halo}} \left( \frac{M_{\text{halo}}}{M_0} \right)^{\alpha(z)}. \quad (1)$$

Here  $x_0(z)$  and  $\alpha(z)$  are “free functions”, whose values are found by the requirement that the resulting luminosity function agrees with observations. As explained in the Appendix, our model has one free parameter, the lifetime  $t_Q$ , which uniquely determines  $x_0(z)$  and  $\alpha(z)$  in any given background cosmology. We assume the background cosmology to be either flat ( $\Lambda$ CDM) with  $(\Omega_\Lambda, \Omega_m, h, \sigma_{8h^{-1}}, n) = (0.7, 0.3, 0.65, 1.0, 1.0)$  or open (OCDM) with  $(\Omega_\Lambda, \Omega_m, h, \sigma_{8h^{-1}}, n) = (0, 0.3, 0.65, 0.82, 1.3)$ . In LCDM, we find  $(-\log[x_0/L_\odot M_\odot^{-1}], \alpha) \approx (1, 0.4)$  and

$\approx (-0.2, -0.1)$  for lifetimes of  $t_Q = 10^8$  and  $t_Q = 10^{6.5}$  yr, respectively. Similarly, in OCDM, we find  $(-\log[x_0/L_\odot M_\odot^{-1}], \alpha) \approx (1, 0.25)$  and  $\approx (-0.2, -0.25)$  for these two lifetimes.

In Figure 1, we demonstrate the agreement between the LF computed in our models with the observational data at two different redshifts,  $z = 2$  and  $z = 3$ . For reference, the upper labels in this figure show the apparent magnitudes in the SDSS  $g'$  band, assuming that the intrinsic quasar spectrum is the same as the mean spectrum in the Elvis et al. (1994) quasar sample. The photometric detection threshold<sup>2</sup> of SDSS is  $g' \approx 22.6$ , corresponding to a BH mass of  $\approx 10^8 M_\odot$  at  $z = 3$  and a three times smaller mass at  $z = 2$ . As the figure shows, the overall quality of the fits is excellent; for reference, the dashed lines show the ad-hoc empirical fitting formulae from Pei (1995). Similarly accurate match to the quasar LF is achieved at different redshifts, and in the models assuming an OCDM cosmology. Figure 1 shows, in particular, that the fits obtained from the power-law ansatz adopting either a short (solid lines) or a long (dotted lines) lifetime are nearly indistinguishable; hence modeling the LF by itself does not constrain the quasar lifetime within the limits  $10^{6.5} \text{ yr} \lesssim t_Q \lesssim 10^8 \text{ yr}$ .

Before considering constraints on the lifetime from clustering, it is useful to point out that estimates for both upper and lower limits on  $t_Q$  follow from the observed luminosity function alone.

*Lower limit on  $t_Q$ .* A halo of mass  $M_{\text{halo}}$  is unlikely to harbor a BH more massive than  $\approx 6 \times 10^{-3} (\Omega_b/\Omega_0) M_{\text{halo}} = 6 \times 10^{-4} M_{\text{halo}}$ , where  $\approx 6 \times 10^{-3}$  is the ratio  $M_{\text{bh}}/M_{\text{bulge}}$  found in nearby galaxies (Magorrian et al. 1998) because  $M_{\text{bulge}}$  cannot be larger than  $(\Omega_b/\Omega_0) M_{\text{halo}}$ . This maximal BH could at best emit  $\approx 10\%$  of the Eddington luminosity in the B-band, implying  $L/M_{\text{halo}} \lesssim 3 L_\odot/M_\odot$ . We find (cf. Fig. 7) that our short lifetime model with  $t_Q = 10^{6.5} \text{ yr}$  nearly reaches this limit; models with shorter lifetimes would require unrealistically large  $L/M_{\text{halo}}$  ratios.

*Upper limit on  $t_Q$ .* Long lifetimes, on the other hand, require the ratio  $L/M_{\text{halo}}$  to be small; this can lead to unrealistically large halo masses. The brightest quasars detected at redshifts  $z \approx 2-3$  have luminosities as large as  $L \approx 10^{14} L_\odot$  (Pei 1995). We find (cf. Fig. 7) that in order to avoid the host halo masses of these bright quasars to exceed  $\sim 10^{15} M_\odot$ , the lifetime cannot be longer than  $\sim 10^8 \text{ yr}$ . An alternative, standard argument goes as follows. The black hole mass grows during the quasar phase as  $e^{t_Q/t_E}$  where  $t_E = 4 \times 10^7 (\epsilon/0.1) \text{ yr}$  is the Eddington time. Assuming a conservative initial black hole mass of  $1 M_\odot$ , a lifetime longer than  $10^9 \text{ yr}$  would give final black hole masses that are unacceptably large.

## 3. THE CLUSTERING OF QUASARS

As demonstrated in the previous section, equally good fits can be obtained to the luminosity function of quasars, assuming either a short or a long lifetime, and a power-law dependence of the mean quasar luminosity on the halo mass  $\bar{L} \propto M^\alpha$ . In this section, we derive the clustering of

<sup>2</sup>See [http://www.sdss.org/science/tech\\_summary.html](http://www.sdss.org/science/tech_summary.html).

quasars in our models, and demonstrate that they depend significantly on the assumed lifetime.

The halos are a biased tracer of the underlying mass distribution, customarily expressed by  $P_{\text{halo}}(k) = b^2 P(k)$  where  $P_{\text{halo}}$  and  $P$  are the halo and mass power spectra as a function of wavenumber  $k$ . The bias parameter for halos of a given mass  $M$  at a given redshift  $z$  is given by (Mo & White 1996)

$$b(M, z) = 1 + \frac{1}{\delta_c} \left[ \left( \frac{\delta_c}{\sigma(M)D(z)} \right)^2 - 1 \right], \quad (2)$$

where  $D(z)$  is the linear growth function,  $\sigma(M)$  is the r.m.s. mass fluctuation on mass-scale  $M$  (using the power spectrum of Eisenstein & Hu 1999), and  $\delta_c \approx 1.68$  is the usual critical overdensity in the Press-Schechter formalism (see Jing 1999 and Sheth & Tormen 1999 for more accurate expressions for  $b(M, z)$  for low  $M$ , which we find not to affect our results here). The bias associated with quasars with luminosity  $L$  in our models is given by averaging over halos of different masses associated with this luminosity. Following equation 19, we obtain

$$b(L, z) \left[ \frac{d\phi}{dL}(L, z) \right]^{-1} \times \int_0^\infty dM \frac{dN}{dM}(M, z) \quad (3)$$

$$b(M, z) \frac{dg}{dL}(L, \bar{L}_{M,z}) f_{\text{on}}(M, z).$$

We show in Figure 2 the resulting bias parameter  $b(L, z)$  in the models corresponding to Figure 1, with short and long lifetimes, and at redshifts  $z = 2$  and 3. As expected, quasars are more highly biased in the long lifetime model, by a ratio  $b(\text{long})/b(\text{short}) \gtrsim 2$ . In the  $\Lambda$ CDM case, at the detection threshold of SDSS, we find  $b(\text{long}) \approx 3$  at  $z = 3$  and  $b(\text{long}) \approx 2$  at  $z = 2$ . Bright quasars with  $g' = 17$  are predicted to have a bias at  $z = 3$  as large as  $b = 10$ . For reference, we also show in this figure the bias parameters obtained in the OCDM cosmology, which are significantly lower than in the  $\Lambda$ CDM case. The number of quasars observed at a fixed flux implies an intrinsically larger number of sources if OCDM is assumed, because the volume per unit redshift and solid angle in an open universe is smaller. This lowers the corresponding halo mass and therefore the bias.

#### 4. COMPARISON WITH AVAILABLE DATA

As emphasized in § 1, the presently available data leave considerable uncertainties in the clustering of quasars. Nevertheless, it is interesting to contrast the results of the previous section with preliminary results from the already relatively large, homogeneous sample of high-redshift quasars in the 2dF survey (Boyle et al. 2000). Our predictions are obtained by relating the apparent magnitude limit to a minimum absolute luminosity at a given redshift:  $\log[L_{\text{min}}(z)/L_{B,\odot}] = 0.4[5.48 - B + 5 \log(d_L(z)/\text{pc}) - 5]$ . This relation assumes no K-correction, justified by the nearly flat quasar spectra ( $\nu F_\nu = \text{const}$ ) at the relevant wavelengths (e.g. Elvis et al. 1994; Pei 1995). In our model, the correlation length  $r_0$  is given implicitly by

$$\xi_q(r_0) \equiv \bar{b}^2(z) D^2(z) \xi_m(r_0) = 1, \quad (4)$$

where  $\xi_m(r)$  is the usual dark matter correlation function, and  $\bar{b}(z)$  is the value of the bias parameter  $b(L, z)$  as determined in the previous section, but now averaged over all quasars with magnitudes brighter than the detection limit,

$$\bar{b}(z) = \left[ \int_{L_{\text{min}}(z)}^\infty dL \frac{d\phi}{dL} \right]^{-1} \int_{L_{\text{min}}(z)}^\infty dL \frac{d\phi}{dL} b(L, z). \quad (5)$$

In Figure 3 we show the resulting correlation lengths in the long and short lifetime models. Also shown is a preliminary data-point with  $1\sigma$  error-bars from the 2dF survey, based on  $\approx 3000$  quasars with apparent magnitudes  $B < 20.85$  (Croom et al. 1999). The upper panel shows the results in our fiducial  $\Lambda$ CDM model with predictions for this magnitude cut. The published results for  $r_0$  are cosmology dependent, and we have simply converted them for our cosmological models by taking the corresponding average of the redshift-distance and angular-diameter-distance – this crude treatment is adequate given the large measurement errors. Our models generically predict a gradual increase of the correlation length with redshift (“positive evolution”). The clustering is dominated by the faintest quasars near the threshold luminosity; as a result, the fixed magnitude-cut of  $B = 20.85$  corresponds to more massive, and more highly clustered halos at higher redshifts. There are two additional effects that determine the redshift-evolution of clustering: (1) quasars of a fixed luminosity are more abundant towards high- $z$ , requiring smaller halo masses to match their number density, and (2) halos with a fixed mass are more highly clustered towards high- $z$ . We find, however, that these effects are less important than the increase in  $M_{\text{halo}}$  caused by fixing the apparent magnitude threshold, which gives rise to the overall positive evolution.

The clustering in the long-lifetime model is stronger, and evolves more rapidly than in the short-lifetime case. As we can see, the present measurement error-bars are large – the whole range of life-times from  $10^{6.5}$  to  $10^8$  yr is broadly consistent with the data, to within  $\sim 2\sigma$ . For the  $\Lambda$ CDM model, the 2dF data-point is consistent with a lifetime of around  $10^{7.7 \pm 0.8}$  yr; in the OCDM model the lifetime is somewhat higher,  $10^{8 \pm 0.8}$  yr. It is worth emphasizing here that the constraints on lifetime from clustering depends on the underlying cosmological parameters one assumes, which future large scale structure measurements (from e.g. the microwave background, galaxy surveys and the Lyman- $\alpha$  forest) will hopefully pin down to the accuracy required here.

Lastly, we note that observational results on  $r_0$  are commonly obtained by a fit to the two-point correlation of the form  $\xi(r) = (r/r_0)^{-\gamma}$ . Since  $r_0$  is the correlation length where the correlation is unity, we expect our formalism to begin to fail on such a scale, because neither linear fluctuation growth nor linear biasing holds. On the other hand, it is also unclear whether  $r_0$  as presently measured from a 2-parameter fit to the still rather noisy observed two-point correlation necessarily corresponds to the true correlation length. While our crude comparison with existing data in Figure 3 suffices given the large measurement errors, superior data in the near future demand a more refined treatment, which is the subject of the next section.

## 5. EXPECTATIONS FROM THE SDSS AND 2dF

Although existing quasar clustering measurements still allow a wide range of quasar lifetimes, and do not provide tight constraints on our models, forthcoming large quasar samples from SDSS or the complete 2dF survey are ideally suited for this purpose. Here we estimate the statistical uncertainties on the derived lifetimes, using the three-dimensional quasar power spectrum  $P_Q(k)$  derived from these surveys.

The variance of the power spectrum is computed by

$$\langle \delta P_Q^2(k) \rangle = n_k^{-1} [\bar{b}^2 P(k) + \bar{n}]^2, \quad (6)$$

where the large scale fluctuations are assumed to be Gaussian,  $n_k$  is the number of independent modes,  $\bar{n}$  is the mean number density of observed quasars,  $P_Q(k) = \bar{b}^2 P(k)$  is the quasar power spectrum and  $P(k)$  is the mass power spectrum (Feldman, Kaiser & Peacock 1994). For a survey of volume  $V$ , and a  $k$ -bin of size  $\Delta k$ , we use  $n_k = k^2 \Delta k V / 4\pi^2$ . The fractional variance is therefore  $n_k^{-1} \{1 + 1/[\bar{n} \bar{b} P(k)]\}^2$ . In terms of minimizing this error, increasing the luminosity cut of a survey has the advantage of raising the bias  $\bar{b}$ , but has the disadvantage of decreasing the abundance  $\bar{n}$ . In practice,  $\bar{b}$  changes relatively slowly with mass (slower than  $\bar{b} \propto M$ ) whereas  $\bar{n}$  varies with mass much more rapidly ( $\bar{n} \sim 1/M$ , or steeper if  $M > M_*$ ). As a result, we find that for our purpose of determining the clustering and the quasar lifetime, it is better to include more (fainter) quasars.

The power spectrum  $P_Q(k)$  of quasars in  $\Lambda$ CDM is shown in Figure 4 at two different redshifts near the peak of the comoving quasar abundance,  $z = 2$  and  $z = 3$ . We assume that redshift slices are taken centered at each redshift with a width of  $\Delta z = 0.5$  (which enters into the volume  $V$  above). Results are shown in the long and short lifetime models, together with the expected  $1\sigma$  error bars from SDSS (crosses). Also shown in the lower panel are the expected error bars from 2dF (open squares), which are slightly larger because of the smaller volume (for SDSS, we assume an angular coverage of  $\pi$  steradians, and for 2dF, an area of 0.23 steradians). We do not show error bars for 2dF beyond  $k \sim 0.01$  Mpc/h because larger scales would likely be affected by the survey window. We also only show scales where the mass power spectrum and biasing are believed to be linear.

As these figures show, the long and short  $t_Q$  models are easily distinguishable with the expected uncertainties both from the SDSS and the 2dF data, out to a scale of  $\sim 100$  Mpc. The measurement errors at different scales are independent (under the Gaussian assumption), and hence, when combined, give powerful constraints e.g. formally, even models with lifetimes differing by a few percent can be distinguished with high confidence using the SDSS. However, systematic errors due to the theoretical modeling are expected to be important at this level, which we will discuss in §7.

In Figure 4, we have used the magnitude cuts for spectroscopy, i.e.  $B = 20.85$  for 2dF and  $B = 20.4$  ( $g' \approx 19$ ) for SDSS. If photometric redshifts of quasars are sufficiently accurate, the magnitude cuts can be pushed fainter, further decreasing the error-bars – although it is likely that

the photometric redshift errors will be large enough that one can only measure the clustering in projection, in some well-defined redshift-bin picked out using color information. Color selection of  $z > 3$  quasars has already proven to be highly effective (Fan et al. 1999); a high redshift sample can give valuable information on the evolution of the quasar clustering (see Fig. 3).

## 6. QUASAR CLUSTERING IN X-RAY

Both the luminosity function (e.g. Miyaji et al. 2000), and the clustering of quasars (e.g. Carrera et al. 1998) has been studied in the X-ray band, analogously to the optical observations described above. At present, the accuracy of both quantities are inferior to that in the optical. Nevertheless, it is interesting to consider the clustering of quasars in the X-ray regime, because (1) applying the exercise outlined above to a different wavelength band provides a useful consistency check on our results, (2) observations with the *Chandra X-ray Observatory* (CXO) and *XMM* can potentially<sup>3</sup> probe quasars at redshifts higher than currently reached in the optical, and (3) X-ray observations are free from complications due to dust extinction, although other forms of obscuration are possible (see §7). In addition, we will consider here the auto-correlation of the soft X-ray background (XRB) as another potential probe of quasar clustering and lifetime.

The formalism we presented in § 2 and § 3 is quite general, and we here apply it to the soft X-ray luminosity function (XRLF) from Miyaji et al. (2000). The details of the fitting procedure are given in the Appendix. In analogy with the optical case, we find that the clustering of X-ray selected quasars depends strongly on the lifetime. As an example, including all quasars whose observed flux is above  $3 \times 10^{-14}$  erg cm<sup>-2</sup> s<sup>-1</sup>, we find the correlation length at  $z = 2$  to be  $\approx 4h^{-1}$  Mpc in the short lifetime, and  $\approx 11h^{-1}$  Mpc in the long lifetime case ( $\Lambda$ CDM). Current data probes the clustering of X-ray quasars only at low redshifts ( $z \lesssim 1$ , see Carrera et al. 1998), where our models suffer from significant uncertainties due to the subhalo problem discussed in §7. Constraints at  $z \gtrsim 2$  could be available in the future from CXO and XMM, provided that a large area of the sky is surveyed at the improved sensitivities of these instruments.

We next focus on the quasar contribution to the soft X-ray background and its auto-correlation, which as we will see is dominated by quasar contributions at somewhat higher redshifts. The mean comoving emissivity at energy  $E$  from all quasars at redshift  $z$ , typically in units of keV cm<sup>-3</sup> s<sup>-1</sup> sr<sup>-1</sup>, is given in our models by

$$\bar{j}(E, z) = \frac{1}{4\pi} \int_0^\infty dL \frac{d\phi}{dL} L_X(E, L), \quad (7)$$

where  $L_X(E, L)$  is the luminosity (in keV s<sup>-1</sup> keV<sup>-1</sup>) at the energy  $E$  of a quasar whose luminosity at  $(1+z)$  keV is  $L$ . We have used the mean spectrum of Elvis et al. (1994) to include a small K-correction when computing the background at observed energies  $E \neq 1$  keV. The mean background is the integral of the emissivity over redshift,

$$\bar{I}(E) = \int_0^\infty \frac{d\chi}{(1+z)} \bar{j}(E_z, \chi), \quad (8)$$

<sup>3</sup>see <http://asc.harvard.edu> and <http://xmm.vilspa.esa.es>, respectively

where  $\bar{I}$  is typically given in units of  $\text{keV cm}^{-2} \text{s}^{-1} \text{sr}^{-1} \text{keV}^{-1}$ ,  $E_z = E(1+z)$ , and  $\chi$  is the comoving distance along the line of sight.

If  $\delta(z)$  is the mass fluctuation at some position at redshift  $z$ , then the fluctuation of the emissivity at the same position and redshift is given by  $b_X(z)\delta(z)\bar{j}(E_z, z)$ , where we have defined the X-ray emission-weighted bias  $\bar{b}_X(z)$  as

$$\bar{b}_X(z) = \frac{1}{\bar{j}(E_z, z)} \frac{1}{4\pi} \int_0^\infty dL \frac{d\phi}{dL} L_X(E_z, L) b_X(L, z). \quad (9)$$

For simplicity, we compute the auto-correlation  $w_\theta$  of the XRB using the Limber approximation, together with the small angle approximation, as:

$$C_\ell(E) = \bar{I}(E)^{-2} \int \frac{d\chi}{r_\chi^2} W^2(E_\chi, \chi) P_0(\ell/r_\chi) \quad (10)$$

$$w_\theta(E) = \int \frac{\ell d\ell}{2\pi} C_\ell(E) J_0(\ell\theta),$$

where  $C_\ell$  is the angular power spectrum,  $J_0$  is the zeroth order Bessel function,  $P_0(\ell/r_\chi)$  is the linear mass power spectrum today,  $r_\chi$  is the angular diameter distance ( $= \chi$  for a flat universe), and  $W(E_\chi, \chi) = \bar{j}(E_z, z)\bar{b}_X(z)D(z)/(1+z)$ . When the power spectrum is measured in practice, shot-noise has to be subtracted or should be included in the theoretical prediction, whereas the same is not necessary for the angular correlation except at zero-lag.

Our models predicts the correct mean background spectrum  $\bar{I}(E)$ , computed from equation 8, at  $E = 1 \text{ keV}$ . We have included all quasars down to the observed  $1 \text{ keV}$  flux of  $2 \times 10^{-17} \text{ erg cm}^{-2} \text{s}^{-1}$ , i.e. we used our models to extrapolate the XRLF to two orders of magnitude fainter than the ROSAT detection threshold for discrete sources (Hasinger & Zamorani 1997), to make up the remaining  $\sim 50\%$  of the XRB at  $1 \text{ keV}$ . Our models predict a faint-end slope that is steeper than the Miyaji et al. (2000) fitting formulae, allowing faint quasars to contribute half of the background. The emissivities peak at  $z \approx 2$ , coinciding with the peak of the XRLF, implying that our model produces most of the XRB, as well as its auto-correlation signal at  $z \approx 2$ . Note that the known contribution from nearby galaxy clusters is  $\sim 10\%$  (Gilli et al. 1999), which we ignore here.

In Figure 5, we show our predictions for the two point angular correlation  $w_\theta$  of the XRB from quasars at  $1 \text{ keV}$ . Most measurements at the soft X-ray bands have yielded only upper limits, which are consistent with our predictions (e.g. variance at  $\lesssim 0.12$  at a scale of  $10 \text{ arcmin}$ . and  $E = 0.9 - 2 \text{ keV}$ , from Carrera et al. 1998; see also references therein). Soltan et al. (1999) obtained angular correlations significantly higher than previous results (dashed curve), which, taken at face value, would imply quasar lifetimes  $t_Q \gg 10^8 \text{ yr}$ . However, the results of Soltan et al. (1999) could be partially explained by galactic contamination (Barcons et al. 2000). We therefore view this measurement as an upper limit, which is consistent with models using both lifetimes we considered. Figure 5 shows that  $w_\theta$  predicted in the long and short lifetime models differ by a factor of  $\sim 2$  on angular scales of  $0.1-1 \text{ degrees}$ ,

offering another potential probe of quasar lifetimes, provided that  $w_\theta$  can be measured more accurately in the future, and that the contribution to the clustering signal from nearby non-quasar sources (e.g. clusters) is small or can be subtracted out. Finally, we note that there have been detections of clustering on several-degree-scales at the hard X-ray bands ( $2-10 \text{ keV}$ ) from the HEAO satellite (Treyer et al. 1998) – while a prediction for such energies would be interesting (see also Lahav et al. 1997), it would require an extrapolation of the X-ray spectrum, since we normalize by fitting to the soft-Xray luminosity function.

## 7. FURTHER CONSIDERATIONS

We have shown above that the quasar lifetime could be measured to high precision, using the soon available large samples of quasars at  $z \lesssim 3$ ; either from the 2dF or the SDSS survey. This precision, however, reflects only the statistical errors in the simple model we have adopted for relating quasars to dark matter halos. The main hindrance in determining the quasar lifetime will likely be systematic errors; here we discuss how several potential complications could affect the derived lifetime.

*Obscured sources.* Considerations of the hard X-ray background have led several authors to suggest the presence of a large population of “absorbed” quasars, necessary to fit the hard slope and overall amplitude of the background. Although not a unique explanation for the XRB, this would imply that the true number of quasars near the faint end of both the optical and soft X-ray LF is  $\sim 10$  times larger than what is observed;  $90\%$  being undetected due to large absorbing columns of dust in the optical, and neutral hydrogen in the soft X-rays (see, e.g. Gilli et al. 1999). Unless the optically bright and dust-obscured phases occur within the same object (Fabian & Iwasawa 1999), this increase would have a direct effect on our results, since we would then need to adjust our fitting parameters to match a  $\sim 10$  times higher quasar abundance. We find that this is easily achieved by leaving  $x_0$  and  $\alpha$  unchanged, and instead raising the lifetime from  $10^{6.5}$  to  $10^{7.5} \text{ yr}$  in the short lifetime model, and from  $10^8$  to  $10^{8.6} \text{ yr}$  in the long lifetime model. In the latter case, a 10-fold increase in the duty cycle requires only an increase in  $t_Q$  by a factor of  $\approx 4$ , owing to the shape of the age distribution  $dp_a/dt$  (Lacey & Cole 1993). Our results would then hold as before, but they would describe the two cases of  $t_Q = 10^{7.5}$  and  $10^{8.6} \text{ yr}$ . Interestingly, this scenario would imply that the quasar lifetime could not be shorter than  $t_Q \approx 10^{7.5} \text{ yr}$ , simply based on the abundance of quasars (cf. § 2). Future infrared and hard X-ray observations should help constrain the abundance of obscured sources, and reduce this systematic uncertainty.

*Multiple BH's in a single halo.* A possibility that could modify the simple picture adopted above is that a single halo might host several quasar black holes. A massive (e.g.  $10^{14} M_\odot$ ) halo corresponds to a cluster of galaxies; while the Press-Schechter formalism counts this halo as a single object. If quasar activity is triggered by galaxy-galaxy mergers, a massive Press-Schechter halo, known to contain several galaxies, could equally well host several quasars (e.g. Cavaliere & Vittorini 1998). There is some observational evidence of perhaps merger driven double quasar

activity (Owen et al. 1985; Comins & Owen 1991). One could therefore envision that quasars reside in the sub-halos of massive “parent” halos – a scenario that would modify the predicted clustering. To address these issues in detail, one needs to know the mass-function of sub-halos within a given parent halo, as well as the rate at which they merge and turn on. In principle, this information can be extracted from Monte Carlo realizations of the formation history of halos in the extended Press–Schechter formalism (i.e. the so called merger tree) together with some estimate of the time-scale for mergers of sub-halos based on, for instance, dynamical friction (e.g. Kauffmann & Haehnelt 2000). Here, we consider two toy models that we hope can bracket the plausible range of clustering predictions.

To simplify matters, we ignore the scatter in  $L$ – $M$  in the following discussion. Suppose one is interested in quasars of a luminosity  $L$  at redshift  $z_0$ , which correspond to Press-Schechter halos of mass  $M_0$  in our formalism as laid out in §2. This choice of  $M_0$  matches the abundance of quasars, expressed approximately as  $L(d\Phi/dL) \approx M_0[dN(M_0, z_0)/dM_0](t_Q/t_{\text{Hub}})$  (the merger, or activation rate of halos is approximated as  $\sim t_{\text{Hub}}^{-1}$ , where  $t_{\text{Hub}}$  is the Hubble time), and implies the bias  $b_0(L) \approx b(M_0, z_0)$ .

In model A, we suppose the Press-Schechter halos are identified at some earlier redshift  $z_1$  – these would be sub-halos of those Press-Schechter halos identified at  $z_0$ . Quasars of luminosity  $L$  now correspond to sub-halos of mass  $M_1$ . The abundance of these sub-halos is given by the Press-Schechter mass function  $dN(M_1, z_1)/dM_1$ , which is related to the mass function at  $z_0$  by  $dN(M_1, z_1)/dM_1 = \int_{M_1}^{\infty} dM [dN(M, z_0)/dM] [dN(M_1, z_1|M, z_0)/dM_1]$  where  $dM_1 \times dN(M_1, z_1|M, z_0)/dM_1$  is the average number of  $M_1 \pm dM_1/2$  sub-halos within parent halos of mass  $M$ , given by (e.g. Sheth & Lemson 1999)

$$\begin{aligned} dN(M_1, z_1|M, z_0)/dM_1 = & \quad (11) \\ \frac{M}{M_1} \frac{1}{\sqrt{2\pi}} \frac{\delta_1 - \delta_0}{[\sigma^2(M_1) - \sigma^2(M)]^{3/2}} \\ \exp \left\{ -\frac{(\delta_1 - \delta_0)^2}{2[\sigma^2(M_1) - \sigma^2(M)]} \right\} \frac{d\sigma^2(M_1)}{dM_1}, \end{aligned}$$

where  $\delta_1 = \delta_c/D(z_1)$  and  $\delta_0 = \delta_c/D(z_0)$  (see eq. 2).

To match the abundance of quasars at luminosity  $L$ , we impose the condition that  $M_1[dN(M_1, z_1)/dM_1] \approx M_0[dN(M_0, z_0)/dM_0]$ , which determines  $M_1$  given  $z_1$ ,  $M_0$  and  $z_0$ . The bias of the quasars is no longer  $b_0(L) \approx b(M_0, z_0)$ , but is instead given by

$$\begin{aligned} b_{\text{eff}}^A(L, z_1) = & \left[ \frac{dN(M_1, z_1)}{dM_1} \right]^{-1} \\ & \int_{M_1}^{\infty} dM \frac{dN(M, z_0)}{dM} \frac{dN(M_1, z_1|M, z_0)}{dM_1} b(M, z_0). \end{aligned} \quad (12)$$

We show in Fig. 6 the ratio of  $b_{\text{eff}}^A(L, z_1)/b_0(L)$  as a function of  $z_1$ , for  $z_0 = 3$  and  $z_0 = 2$  respectively, and for a range of masses  $M_0$  which are representative of the halos that dominate our clustering signal in previous discussions. It is interesting how the bias  $b_{\text{eff}}^A(L, z_1)$  is not

necessarily larger than our original bias  $b_0(L)$ , despite the fact that the bias of sub-halos should be boosted by their taking residence in bigger halos. This is because the relevant masses here (e.g.  $M_0$ ) are generally large, and we find that the number of halos of mass  $M_0$  at  $z_1$  is always *smaller* than the number of halos of the same mass at  $z_0 < z_1$ . Hence, to match the observed abundance of quasars at the same  $L$ ,  $M_1$  must be chosen to be smaller than  $M_0$ . As Fig. 6 shows, this could, in some cases, more than compensate the increase in clustering due to massive parent halos. Because of these two opposing effects, the bias does not change by more than about 50% even if one considers  $z_1$  as high as 10. This translates into a factor of  $\sim 2$  uncertainty in our predictions for the quasar power spectrum. Our clustering predictions for the short and long lifetime models differ by about a factor of  $\sim 5$ , implying that the lifetime can still be usefully constrained at  $z \gtrsim 2$ . As we can see from Fig. 6, at lower redshifts, or equivalently lower  $M_0/M_*$ , our predictions for the quasar power spectrum should be more uncertain.

One might imagine modifying the above model by allowing mergers to take place preferentially in massive parents, and therefore boosting the predicted bias. In model B, we adopt a more general procedure of matching the observed quasar abundance by  $L(d\Phi/dL) = M_1 \int_{M_1}^{\infty} dM [dN(M, z_0)/dM] [dN(M_1, z_1|M, z_0)/dM_1] (t_Q/t_{\text{Hub}}) f(M_1, M)$  where  $(t_Q/t_{\text{Hub}}) f(M_1, M)$  is the probability that an  $M_1$  sub-halo residing within a parent halo of  $M_0$  harbors an active quasar of luminosity  $L$ . It is conceivable that  $f$  increases with the parent mass  $M_0$  – a more massive parent might encourage more quasar activity by having a higher fraction of mergers or collisions. The following heuristic argument shows that one might expect  $[dN(M_1, z_1|M, z_0)/dM_1] f(M_1, M)$  to scale approximately as  $\sim M^{4/3}$ . Let  $N_h$  be the number of sub-halos inside a parent halo of mass  $M$ . The rate of collisions is given by  $N_h^2 v_h \sigma_h / R^3$  where  $v_h$  is the velocity of the sub-halos,  $\sigma_h$  is their cross-section and  $R^3$  is the volume of the parent halo. Using  $N_h \propto M$  (which can be obtained from eq. 11 in the large  $M$  limit),  $v_h \propto \sqrt{M/R}$  (virial theorem) and  $R^3 \propto M$  (fixed overdensity of  $\sim 200$  at the redshift of formation), the rate of collisions scales with the parent mass as  $M^{4/3}$ , if one ignores the possibility that  $\sigma_h$  might depend on the parent mass as well. A similar scaling of  $M^{1.3}$  has been observed in simulations of the star-burst model for Lyman-break objects (Kolatt et al. 1999, Weschler et al. 1999).

To model the enhanced rate of collisions inside massive parent halos, we can simply modify model A by using  $f(M_1, M) = (M/M_1)^{1/3}$ . The effective bias is given by

$$\begin{aligned} b_{\text{eff}}^B(L, z_1) = & \quad (13) \\ & \left[ \int_{M_1}^{\infty} dM \frac{dN(M, z_0)}{dM} \frac{dN(M_1, z_1|M, z_0)}{dM_1} \left( \frac{M}{M_1} \right)^{\frac{1}{3}} \right]^{-1} \\ & \times \int_{M_1}^{\infty} dM \frac{dN(M, z_0)}{dM} \frac{dN(M_1, z_1|M, z_0)}{dM_1} \left( \frac{M}{M_1} \right)^{\frac{1}{3}} b(M, z_0). \end{aligned}$$

We find that the above prescription does not significantly alter our conclusions following from model A: the

$M^{1/3}$  enhancement of the activation rate inside massive parent halos turns out to be relatively shallow, and translate to a small effect in the bias. Finally, we note that  $z_1$  above could in principle depend on  $M_0$  and  $M_1$ , a possibility that would require further modeling and is not pursued here.

*Galaxies without BH's.* Another possibility that could modify our picture is that only a fraction  $f < 1$  of the halos harbor BH's; the duty cycle could then reflect this fraction, rather than the lifetime of quasars. Although there is evidence (e.g. Magorrian et al. 1998) that most *nearby* galaxies harbor a central BH, this is not necessarily the case at redshifts  $z = 2 - 3$ : the fraction  $f$  of galaxies hosting BH's at  $z = 2 - 3$  could, in principle have merged with the fraction  $1 - f$  of galaxies without BH's, satisfying the local constraint.

Using the extended Press-Schechter formalism (Lacey & Cole 1993), one can compute the rate of mergers between halos of various masses. On galaxy-mass scales, the merger rates at  $z = 2 - 3$  are comparable to the reciprocal of the Hubble time (cf. Fig. 5 in Haiman & Menou 2000), implying that a typical galaxy did not go through numerous major mergers between  $z = 2 - 3$  and  $z = 0$ , i.e. that the fraction  $f$  cannot be significantly less than unity at  $z = 2 - 3$ . A more detailed consideration of this issue is beyond the scope of this paper; we simply note that the lifetimes derived here scale approximately as  $1/f$ , where  $f$  is likely of order unity.

*Larger scatter in  $L/M$ .* The scatter  $\sigma$  we assumed around the mean relation between quasar luminosity and halo mass is motivated by the scatter found empirically for the  $M_{\text{bh}} - M_{\text{bulge}}$  relation (Magorrian et al. 1998). It is interesting to consider the sensitivity of our conclusions to an increased  $\sigma$ . In general, scatter raises the number of quasars predicted by our models, by an amount that depends on the slope of the underlying mass function  $dN/dM$ . As a result, increasing  $\sigma$  raises, and flattens the predicted LF. We find that an increase of  $\sigma$  from 0.5 to 1 (an additional order of magnitude of scatter) can be compensated by a steeper  $\bar{L}_M$  relation, typically replacing  $\alpha$  with  $\approx \alpha - 0.5$ . As a result of the increase in  $\sigma$ , quasars with a fixed  $L$  are, on average, associated with larger, and more highly biased halos.

Nevertheless, we find that the mean bias  $\bar{b}$  of all sources above a fixed flux (cf. eq. 5), and therefore the correlation length  $r_0$ , is unchanged by the increased scatter (at the level of  $\sim 3\%$ ). The reason for the insensitivity of  $r_0$  to the amplitude of the scatter can be understood as follows. The mean bias  $\bar{b}$  of all sources with  $L > L_{\text{min}}$  is dominated by the bias  $b(L)$  of sources near the threshold  $L_{\text{min}}$ . The latter is obtained by averaging  $b(M)$  over halos of different masses (cf. eq. 4), and it is dominated by the bias of the smallest halos within the width of the scatter, i.e. of halos with mass  $M_{\text{min}} \approx \bar{M}/10^\sigma$ , where  $\bar{M}$  defines the mean relation between  $L_{\text{min}}$  and halo mass i.e.  $L_{\text{min}} = \bar{L}(\bar{M})$ , and  $\sigma$  quantifies the scatter (see eq. 16). As mentioned before, increasing the scatter makes the luminosity function flatter, which means to match the observed abundance of halos at a fixed luminosity  $L_{\text{min}}$ , one has to choose a higher  $\bar{M}$ . In other words,  $\bar{M}$  scales up with the scatter, and it turns out to scale up approximately as  $10^\sigma$ , making

$M_{\text{min}}$  and hence the effective bias roughly independent of scatter.

We note that the relation between quasar luminosity and halo mass can, in principle be derived from observations, by measuring  $M_{\text{halo}}$  for the hosts of quasars (e.g. by weak lensing, or by finding test particles around quasars, such as nearby satellite galaxies).

*Mass and redshift dependent lifetime.* In all of the above, we have assumed that the quasar lifetime is a single parameter, independent of the halo mass. This is not unreasonable if the Eddington time, the timescale for the growth of black hole mass, is indeed the relevant timescale,  $4 \times 10^7 (\epsilon/0.1)$  yr. Implicit in such reasoning is that the active phase of the quasar is coincident with the phase where the black hole gains most of its mass. This is not the only possibility; see Haehnelt et al. (1999) for more discussions. One can attempt to explore how  $t_Q$  depends on halo mass by applying our method to quasars grouped into different absolute luminosity ranges, but the intrinsic scatter in the mass-luminosity relation should be kept in mind. We emphasize, however, since we fit the luminosity function and clustering data at the same redshift, there is no need within our formalism to assume a redshift independent lifetime. In fact, performing our exercise as a function of redshift could give interesting constraints on how  $t_Q$  evolves with redshift.

## 8. CONCLUSIONS

In this paper, we have modeled the quasar luminosity function in detail in the optical and X-ray bands using the Press-Schechter formalism. The lifetime of quasars  $t_Q$  enters into our analysis through the duty-cycle of quasars, and we find that matching the observed quasar LF to dark matter halos yields the constraint  $10^6 \lesssim t_Q \lesssim 10^8$  yr: smaller lifetimes would imply overly massive BH's, while longer lifetimes would necessitate overly massive halos. This range reassuringly brackets the Eddington timescale of  $4 \times 10^7 (\epsilon/0.1)$  yr.

The main conclusion of this paper is that the lifetime (and hence  $\epsilon$ , if the Eddington time is the relevant timescale for quasar activity) can be further constrained within this range using the clustering of quasars: for quasars with a fixed luminosity, longer  $t_Q$  implies larger host halo masses, and higher bias. We find that as a result, the correlation length  $r_0$  varies strongly with the assumed lifetime. Preliminary data from the 2dF survey already sets mild constraints on the lifetime. Depending on the assumed cosmology, we find  $t_Q = 10^{7.7 \pm 0.8}$  yr ( $\Lambda$ CDM) or  $t_Q = 10^{8 \pm 0.8}$  yr (OCDM) to within  $1\sigma$  statistical uncertainty. These values are also found to satisfy upper limits on the auto-correlation function of the soft X-ray background.

Forthcoming large quasar samples from SDSS or the complete 2dF survey are ideally suited for a study of quasar clustering, and they can, in principle constrain the quasar lifetime to high accuracy, with small statistical errors. We expect the modeling of the quasar-halo relation, as well as the possible presence of obscured quasars, to be the dominant sources of systematic uncertainty. Not discussed in depth in this paper is the possibility of using higher moments (such as skewness), which our models also make definite predictions for, and will be considered in a

future publication. Remarkably, our best determination of the lifetime of quasars might come from the statistics of high-redshift quasars, rather than the study of individual objects.

Near the completion of this work, we became aware of a similar, independent study by P. Martini & D. Weinberg. We thank M. Haehnelt, K. Menou, E. Quataert, U.-L. Pen., U. Seljak, R. Sheth and D. Spergel for useful discussions, T. Miyaji for his advice on the X-ray luminos-

ity function, and T. Shanks and S. Croom for discussions on the 2dF survey. Support for this work was provided by the DOE and the NASA grant NAG 5-7092 at Fermilab, by the NSF grant PHY-9513835, by the Taplin Fellowship to LH and by NASA through the Hubble Fellowship grant HF-01119.01-99A to ZH, awarded by the Space Telescope Science Institute, which is operated by the Association of Universities for Research in Astronomy, Inc., for NASA under contract NAS 5-26555.

## REFERENCES

- Andreani, P., & Cristiani, S. 1992, *ApJ*, 398, L13  
 Andredakis, Y. C., & Sanders, R. H. 1994, *MNRAS*, 267, 283  
 Barcons, X., Carrera, F. J., Ceballos, M. T., Mateos, S. 200, in *Proc. of Workshop on Large scale structure in the X-ray Universe*, Santorini, 1999, astro-ph/0001191  
 Boyle, B. J., Smith, R. J., Shanks, T., Croom, S. M., & Miller, L. 1999, in *Cosmological Parameters and the Evolution of the Universe*, Proceedings of the 183rd symposium of the International Astronomical Union held in Kyoto, Japan, August 18-22, 1997, Ed. K Sato, Dordrecht, Boston: Kluwer Academic, p. 178  
 Boyle, B. J., Shanks, T., Croom, S. M., Smith, R. J., Miller, L., Loaring, N., & Heymans, C. 2000, *MNRAS*, in press, astro-ph/0005368  
 Blandford, R. D. 1999, to appear in *Galaxy Dynamics*, ed. Meritt, Valluri and Sellwood, ASP conf. series, astro-ph/9906025  
 Cavaliere, A., & Vittorini, V. 1998, in Proceedings of "The Young Universe: Galaxy Formation and Evolution at Intermediate and High Redshift", Eds S. D'Odorico, A. Fontana, & E. Giallongo, ASP Conf. Ser. 146, 26  
 Carrera, F. J., Barcons, X., Fabian, A. C., Hasinger, G., Mason, K. O., McMahon, R. G., Mittaz, J. P. D., & Page, M. J. 1998, *MNRAS*, 299, 229  
 Cattaneo, A., Haehnelt, M. G., & Rees, M. J. 1999, *MNRAS*, 308, 77  
 Comins, N. F., & Owen, F. N. 1991, *ApJ*, 382, 108  
 Croom, S. M., & Shanks, T. 1996, *MNRAS*, 281, 893  
 Croom, S. M., Shanks, T., Boyle, B. J., Smith, R. J., Miller, L., & Loaring, N. S. 1999, in "Redshift Surveys and Cosmology", held at Dunk Island, 24-28 August 1999, Ed. M. Colless, <http://www.mso.anu.edu.au/DunkIsland/Proceedings>  
 Efstathiou, G., & Rees, M. J. 1988, *MNRAS*, 230, 5p  
 Eisenstein, D. J., & Loeb, A. 1996, 459, 432  
 Elvis, M., Wilkes, B. J., McDowell, J. C., Green, R. F., Bechtold, J., Willner, S. P., Oey, M. S., Polomski, E., & Cutri, R. 1994, *ApJS*, 95, 1  
 Fan, X., et al. 1999, *AJ*, 118, 1  
 Feldman, H. A., Kaiser, N., & Peacock, J. A. 1994, *ApJ*, 426, 23  
 Gilli, R., Risaliti, G., & Salvati, M. 1999, *AA*, 347, 424  
 Haehnelt, M. G., Natarajan, P. & Rees, M. J. 1998, *MNRAS*, 300, 817  
 Haiman, Z., & Loeb, A. 1998, *ApJ*, 503, 505  
 Haiman, Z., & Menou, K. 2000, *ApJ*, in press  
 Hasinger, G., & Zamorani, G. 1997, in "Festschrift for R. Giacconi's 65th birthday", World Scientific Publishing Co., H. Gursky, R. Ruffini, L. Stella eds., in press, astro-ph/9712341  
 Iovino, A., & Shaver, P. A. 1988, *ApJ*, 330, L13  
 Iovino, A., Shaver, P. A., & Cristiani, S. 1991, in *ASP Conf Ser.* 21, ed. D. Crampton (San Francisco: ASP), p. 202.  
 Jing, Y. P. 1999, *ApJ*, 515, L45  
 Kaiser, N. 1984, *ApJ*, 284, L9  
 Kauffmann, G., & Haehnelt, M. 2000, *MNRAS*, 311, 576  
 Kauffmann, G., & White, S. D. M. 1993, *MNRAS*, 261, 921  
 Kolatt, T. S., et al. 1999, *ApJ*, 523, L109  
 La Franca, F., Andreani, P., & Cristiani, S. 1998, *ApJ*, 497, 529  
 Lacey, C., & Cole, S. 1993, *MNRAS*, 262, 627  
 Lahav, O., Piran, T. & Treyer, M. A. 1997, *MNRAS*, 284, 499  
 Lynden-Bell, D. 1967, *MNRAS*, 136, 101  
 Magorrian, J., et al. 1998, *AJ*, 115, 2285  
 Mo, H. J., & White, S. D. M. 1996, *MNRAS*, 282, 347  
 Magorrian, J., et al. 1998, *AJ*, 115, 2285  
 Miyaji, T., Hasinger, G., & Schmidt, M. 2000, *AA*, 353, 25  
 Miyaji, T., Ishisaki, Y., Ogasaka, Y., Ueda Y., Freyberg, M. J., Hasinger, G., & Tanaka, Y. 1998, *A&A* 334, L13  
 Owen, F. N., Odea, C. P., Inoue, M., Eilek, J. A. 1985, *ApJ*, 294, L85  
 Pei, Y. C. 1995, *ApJ*, 438, 623  
 Percival, W. J., & Miller, L. 1999, *MNRAS*, 329, 823  
 Press, W. H., & Schechter, P. L. 1974, *ApJ*, 181, 425  
 Raychaudhury, S., von Braun, K., Bernstein, G. M., & Guhathakurta, P. 1997, *AJ*, 113, 2046  
 Rees, M. J. 1984, *ARA&A*, 22, 471  
 Sabbey, C. N., Oemler, A., Coppi, P., Baltay, C., Bongiovanni, A., Bruzual, G., Garcia, C. E., Musser, J., Rengstorf, A. W., Snyder, J. A. 1999, *ApJ*, submitted, astro-ph/9912108  
 Sheth, R. K. & Lemson, G. 1999, *MNRAS*, 304, 767  
 Sheth, R. K., & Tormen, G. 1999, *MNRAS*, 308, 119  
 Shaver, P. A., et al. 1996, *Nature*, 384, 439  
 Soltan, P. A., Freyberg, M., Hasinger, G., Miyaji, T., Treyer, M., & Trümper, J. 1999, *A&A*, 349, 354  
 Stephens, A. W., Schneider, D., Schmidt, M., Gunn, J. E., & Weinberg, D. H. 1997, *AA*, 114, 41  
 Treyer, M., Scharf, C., Lahav, O., Jahoda, K., Boldt, E. & Piran, T. 1998, *ApJ*, 509, 531  
 van der Marel, R. P. 1999, *AJ* 117, 744  
 Wechsler, R. H., Bullock, J. S., Somerville, R. S., Kolatt, T. S., Primack, J. R., Blumenthal, G. R., & Dekel, A. 1999, in *Clustering at High Redshift*, ASP Conf. Ser., Eds. A. Mazure, O. Le Fevre, & V. Lebrun, in press, astro-ph/9910359

## APPENDIX

In this Appendix, we describe our models for the luminosity function (LF) of quasars, based on associating quasar BHs with dark halos. Our main assumption is that there is, on average, a direct monotonic relation between halo mass and quasar light. Our treatment is similar to previous works (Haiman & Loeb 1998; Haehnelt et al. 1998), but differs in some of the details. We adopt the parameterization of the observational LF in the optical B band, given in the redshift range  $0 < z \lesssim 4$  by Pei (1995). We assume the background cosmology to be either flat ( $\Lambda$ CDM) with  $(\Omega_\Lambda, \Omega_m, h, \sigma_{8h^{-1}}, n) = (0.7, 0.3, 0.65, 1.0, 1.0)$  or open (OCDM) with  $(\Omega_\Lambda, \Omega_m, h, \sigma_{8h^{-1}}, n) = (0, 0.3, 0.65, 0.82, 1.3)$ . The LF quoted by Pei (1995) is scaled appropriately with cosmology by keeping  $(d\phi/dL)dVd_L^2 = \text{const}$ , where  $dV$  is the volume element, and  $d_L$  is the luminosity distance), so that  $(d\phi/dL)dL$  is the comoving abundance in  $\text{Mpc}^{-3}$  of quasars with B-band luminosity  $L$  (in solar units  $L_{B,\odot}$ ). The comoving abundance  $dN/dM(M, z)$  of dark halos is assumed to follow the Press-Schechter (1974) formalism. We assume that each halo harbors a single quasar that turns on when the halo forms, i.e. triggered by merger (e.g. Percival & Miller 1999), and shines for a fixed lifetime  $t_Q$  (relaxing these assumptions is discussed below in section 7). The duty-cycle  $f_{\text{on}}$  of halos with mass  $M$  at redshift  $z$ , is then given by the fraction of these halos younger than  $t_Q$ . The distribution of ages  $dp_a/dt(M, z, t)$  for halos of mass  $M$  existing at redshift  $z$  is obtained using the extended Press-Schechter formalism, which assumes that the halo formed at the epoch when it acquired half of



its present mass (Lacey & Cole 1993). The duty-cycle, which is the probability that a dark matter halo of a given mass harbors an active quasar, is simply

$$f_{\text{on}}(M, z) = \int_0^{t_Q} dt \frac{dp_a}{dt}(M, z, t). \quad (14)$$

A model in which the quasar turns on/off more gradually (as expected if the mass of the BH grows significantly during the luminous quasar phase) is equivalent to one having additional scatter in the ratio  $L/M$ , which is discussed in § 7. We next relate the quasar luminosity to the mass of its host halo. We define  $dp/dL(M, L, z)$  to be the probability that a halo of mass  $M$  at redshift  $z$  hosts a quasar with luminosity  $L$ , and express this quantity as

$$\frac{dp}{dL}(L, M, z) = \frac{dg}{dL}(L, \bar{L}_{M,z}) f_{\text{on}}(M, z). \quad (15)$$

Here  $dg/dL(L, \bar{L}_{M,z})$  is the probability distribution of luminosities associated with the subset of halos of mass  $M$  harboring a live quasar (normalized to  $\int_0^\infty dL dg/dL = 1$ ), and  $\bar{L}_{M,z}$  is the mean quasar luminosity for these halos. In the limit of a perfect intrinsic correlation, we would have  $dg/dL(L, \bar{L}_{M,z}) = \delta(L - \bar{L}_{M,z})$ ; more realistically, this correlation will have non-negligible scatter. Lacking an a-priori theory for this scatter, we here simply assume that it follows the same functional form as the scatter found empirically for the  $M_{\text{bh}} - M_{\text{bulge}}$  relation (Magorrian et al. 1998), and we set

$$\frac{dg}{dL}(L, \bar{L}_M) \propto \exp(-(\log L / \bar{L}_{M,z})^2 / 2\sigma^2). \quad (16)$$

For reference, we note that the empirical scatter between  $M_{\text{bh}}$  and  $M_{\text{bulge}}$  gives  $\sigma \sim 0.5$ , it is not yet clear, however, what fraction of this scatter is intrinsic vs. instrumental (van der Marel 1999). One might expect the scatter in the  $L - M_{\text{halo}}$  relation not to be significantly larger, since (i) for a sufficiently high fueling rate, the luminosity  $L$  corresponding to  $M_{\text{bh}}$  is likely to always be near the Eddington limit, and (ii) at least for disk galaxies, the bulge luminosity correlates well with the total luminosity  $L_{\text{tot}}$  ( $\sigma \sim 0.5$ , see e.g. Andredakis & Sanders 1994);  $L_{\text{tot}}$  is tightly correlated with the velocity dispersion  $\sigma_v$  through the Tully-Fisher relation (e.g. Raychaudhury et al. 1997) as is the total halo mass to  $\sigma_v$  (Eisenstein & Loeb 1996). Nevertheless, in § 7 below we will investigate the consequences of an increased scatter. We note that an extension of the models presented here, by following the merger histories of halos and their BH's can, in principle, be used to estimate the scatter in  $L/M_{\text{halo}}$ . Cattaneo, Haehnelt & Rees (1998) have used this approach to fit the observed relation  $M_{\text{bh}}/M_{\text{bulge}}$ , including its scatter.

Under the above assumptions, the cumulative probability that a halo of mass  $M$  hosts a quasar with luminosity equal to or greater than  $L$  is given by

$$p(L, M, z) = f_{\text{on}}(M, z) \int_L^\infty dL \frac{dg}{dL}(L, \bar{L}_{M,z}), \quad (17)$$

and matching the observed cumulative quasar LF requires

$$\int_L^\infty dL \frac{d\phi}{dL}(L, z) = \int_0^\infty dM \frac{dN}{dM}(M, z) p(L, M, z), \quad (18)$$

or alternatively, matching the differential LF gives

$$\frac{d\phi}{dL}(L, z) = \int_0^\infty dM \frac{dN}{dM}(M, z) \frac{dg}{dL}(L, \bar{L}_{M,z}) f_{\text{on}}(M, z). \quad (19)$$

Equation 18 or 19, together with equations 14, 16, and 17 implicitly determines the function  $\bar{L}_{M,z}$ , once the quasar lifetime  $t_Q$  and magnitude of scatter  $\sigma$  are specified. In general, these equations would need to be solved iteratively. In practice, we have found that sufficiently accurate solutions (given the error bars on the observational LF in Pei 1995; cf. Fig. 1) can be found by using the simple power-law ansatz:

$$\bar{L}_{M,z} = x_0(z) M_{\text{halo}} \left( \frac{M_{\text{halo}}}{M_0} \right)^{\alpha(z)}, \quad (20)$$

where the coefficients  $x_0(z)$  and  $\alpha(z)$  depend on  $t_Q$ ,  $\sigma$ , and the underlying cosmology (Haiman & Loeb 1998; Haehnelt et al. 1998). In summary, assuming a fixed scatter  $\sigma$ , our model has only one free parameter, the quasar lifetime  $t_Q$ .

We emphasize that our parameterization in equation 20 is purely phenomenological – it gives us a convenient way to relate the quasar luminosity to the host halo mass ( $\bar{L}_{M,z}$ ). In reality, the quasar luminosity likely depends on the details of its immediate physical environment (e.g. gas supply, magnetic fields, angular momentum distribution, etc.), in addition to the halo mass. Our description includes these possibilities only in allowing a non-negligible scatter around the mean relation  $\bar{L}_{M,z}$ . The rationale behind this choice is that the average properties of the physical environment should ultimately be governed by the halo mass (or circular velocity), as expected within the picture of structure formation via hierarchical clustering.

A useful check on the physical implications of equation 20 is obtained by assuming that the luminosity  $\bar{L}_{M,z}$  is produced by a BH of mass  $M_{\text{bh}}$ , shining at the Eddington limit  $L_{\text{Edd}} = (4\pi G \mu m_p c / \sigma_T) M_{\text{bh}}$ . In the mean spectrum of a sample of quasars with detections from radio to X-ray bands (Elvis et al. 1994),  $\approx 7\%$  of the bolometric luminosity is emitted in the rest-frame  $B$  band, resulting in  $L = 0.07 L_{\text{Edd}} = 5 \times 10^3 L_{\text{B},\odot} (M_{\text{bh}}/M_{\odot})$ . Equation 20 then translates into a relation between the mass of a BH and its host halo,

$$\bar{M}_{\text{bh}} = 10^{-3.7} x_0(z) M_{\text{halo}} \left( \frac{M_{\text{halo}}}{M_0} \right)^{\alpha(z)}. \quad (21)$$

As an example, Haehnelt et al. (1999) argue that the central BH mass is determined by a radiative feedback from the central BH that would unbind the disk in a dynamical time. Their derived scaling corresponds to  $\alpha = 2/3$  and  $x_0 \propto (1+z)^{5/2}$ , not far from what we find for the long-lifetime case (cf. Figure 7 and discussion below).

In Figure 7, we show the values of the parameters  $x_0(z)$  and  $\alpha(z)$  obtained in our models when two different quasar lifetimes are assumed,  $t_Q = 10^{6.5}$  (solid curves) and  $t_Q = 10^8$  yr (dotted curves). The filled dots show the parameters in  $\Lambda$ CDM, and the empty dots in the OCDM cosmology. We have set the arbitrary constant  $M_0 = 10^{12} M_{\odot}$  in both cases. Note that  $t_Q$  determines both  $\alpha$  and  $x_0$ , and therefore the values of  $\alpha$  and  $x_0$  are correlated. In general, the fitting parameters show little evolution in the range  $2 < z < 4$ , around the peak of the quasar LF. According to equation 21, the corresponding BH masses in, e.g. a  $10^{12} M_{\odot}$  halo at  $2 < z < 4$  are  $M_{\text{bh}} \approx 4 \times 10^{-4} M_{\text{halo}} = 4 \times 10^8 M_{\odot}$  and  $M_{\text{bh}} \approx 2 \times 10^{-5} M_{\text{halo}} = 2 \times 10^7 M_{\odot}$  in the short and long lifetime models, respectively.

The fitting procedure described above can be repeated in the X-ray bands. We therefore fit the XRLF using equation 20 analogously to the optical case, except  $\bar{L}_{M,z}$  now denotes the X-ray luminosity at 1 keV, quoted in units of  $\text{erg s}^{-1}$ . Note that the XRLF in Miyaji et al. (2000) is quoted a function of luminosity at observed 1 keV, i.e. no K-correction is applied (alternatively, the XRLF can be interpreted as the rest-frame luminosity function of sources with an average intrinsic photon index of 2). Figure 8 shows the resulting fitting parameters  $x_0$  and  $\alpha$  in the  $\Lambda$ CDM cosmology, analogous to those shown in Figure 8 for the optical case. It is apparent that both parameters have a somewhat behavior different from that in the optical. This reflects the fact that the mean quasar spectrum must evolve with redshift, or at least is black-hole/halo mass dependent: if every quasar had the same spectrum, or at least a similar X-ray/optical flux ratio, the fitting parameters derived from the optical and X-ray LF would differ only by a constant in  $x_0$ . For our purpose of deriving clustering, it is sufficient to treat  $x_0$  and  $\alpha$  as phenomenological fitting parameters, and we do not address the physical reason for the apparent spectral evolution (see Haiman & Menou for a brief discussion).

It is important to note that the simple power-law ansatz in equation 20 with the parameters shown in Figure 8 adequately fits only the faint end of the XRLF. In the optical case, the entire range of observed luminosities is well matched by our models (cf. Fig 1). In comparison, the well-fitted range in X-rays typically extends from the detection threshold to up to 2-3 orders of magnitude in luminosity (i.e. typically upto  $\sim 3 \times 10^{45} \text{ erg s}^{-1}$ ), depending on redshift, and our models underestimate the abundance of still brighter quasars. One might then consider searching for a different ansatz to replace equation 20 that fits the entire range of the observed LF. However, we have verified that the rare quasars with these high luminosities would contribute negligibly both to the clustering signals, or the XRB investigated here. Therefore, we did not consider further improvements over equation 20, since this would not change our results.

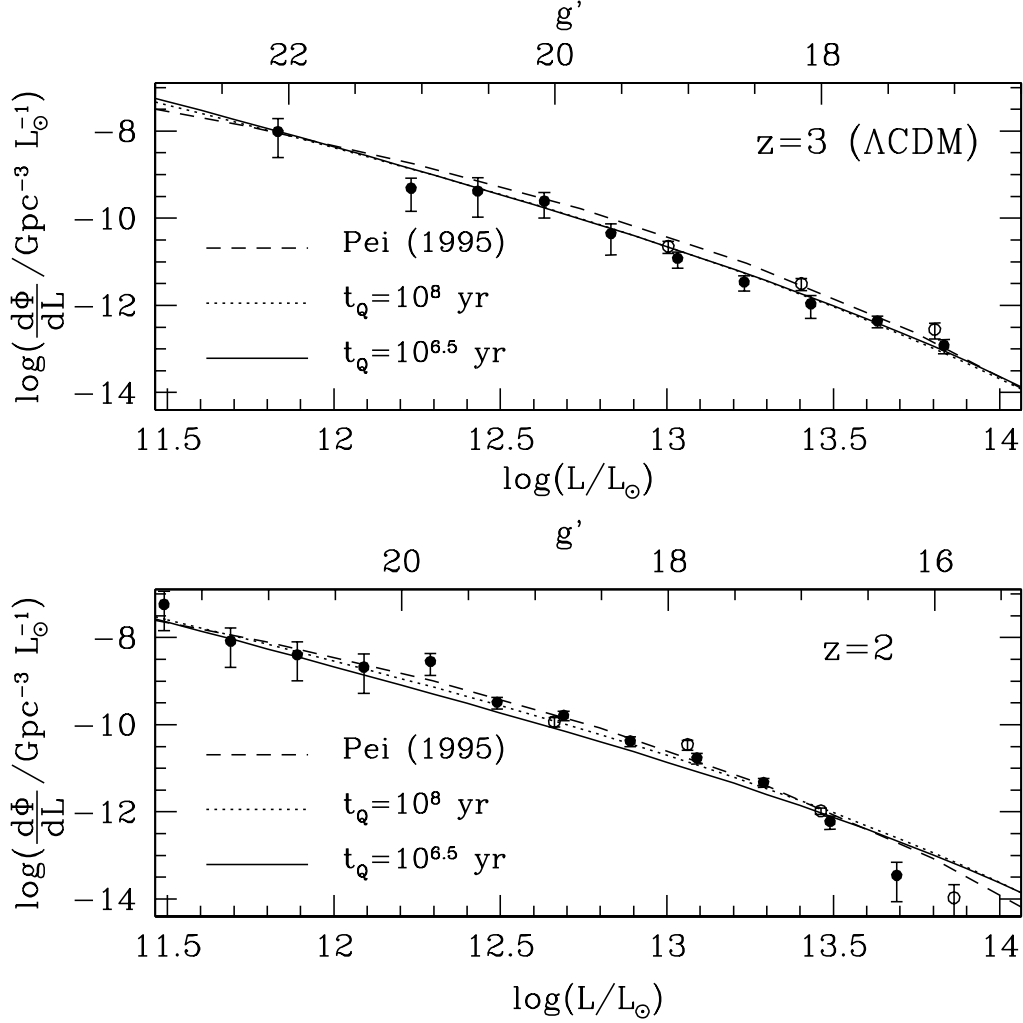


FIG. 1.— Fits to the quasar luminosity function at redshifts  $z = 2$  and  $3$  in our models, with two different quasar lifetimes  $t_Q = 10^{6.5}$  (solid curves) and  $t_Q = 10^8$  yr (dotted curves). Also shown are the data, and fitting function (dashed curves) for the LF from Pei (1995). The quality of our fits at different redshifts or in the OCDM model are similar. The upper labels show the corresponding apparent magnitudes in the SDSS  $g'$  band, assuming that the intrinsic quasar spectrum is the same as the mean spectrum in the Elvis et al. (1994) quasar sample.

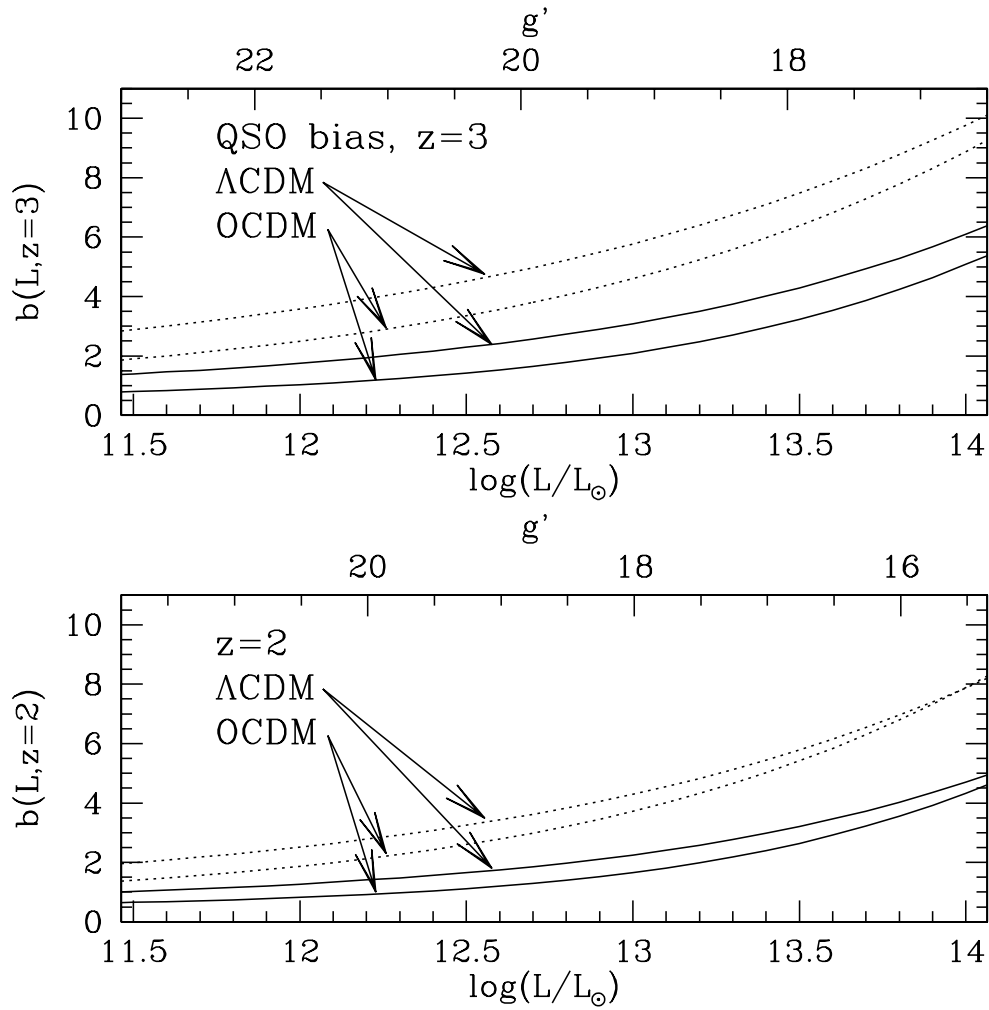


FIG. 2.— Bias parameter  $b(L, z)$  of quasars as a function of their intrinsic B-band luminosity (lower labels) or apparent SDSS  $g'$  magnitude (upper labels), in the models with two different quasar lifetimes  $t_Q = 10^{6.5}$  (solid curves) and  $t_Q = 10^8$  yr (dotted curves) as shown in Figure 1. For comparison, the bias parameter is also shown in the OCDM model. Quasars are more highly biased in the long lifetime models, and in  $\Lambda$ CDM.

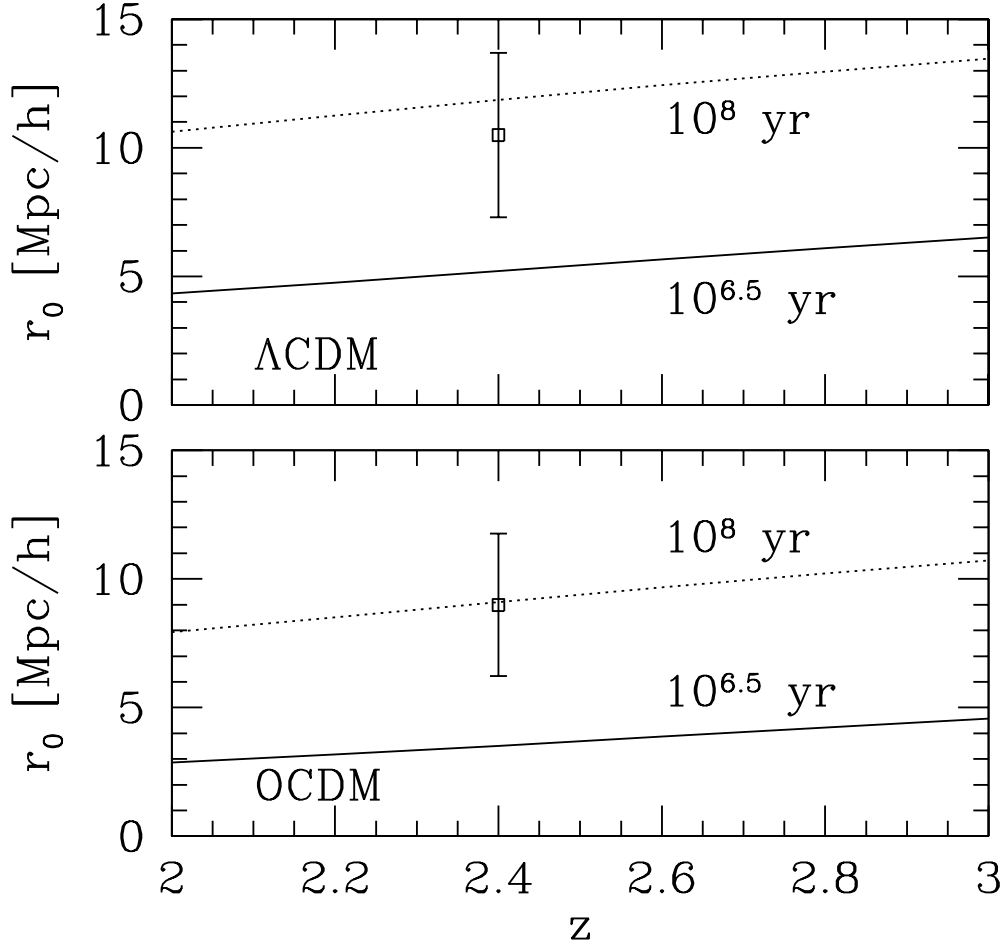


FIG. 3.— Correlation length  $r_0$  in our models with two different quasar lifetimes  $t_Q = 10^{6.5}$  (solid curves) and  $t_Q = 10^8$  yr (dotted curves). An apparent magnitude cut of  $B < 20.85$  was used, corresponding to the limits of the 2dF survey (Croom et al. 1999). The open square shows a preliminary result from 2dF. The upper panel shows our results in the  $\Lambda\text{CDM}$  model, and the lower panel in  $\text{OCDM}$ .

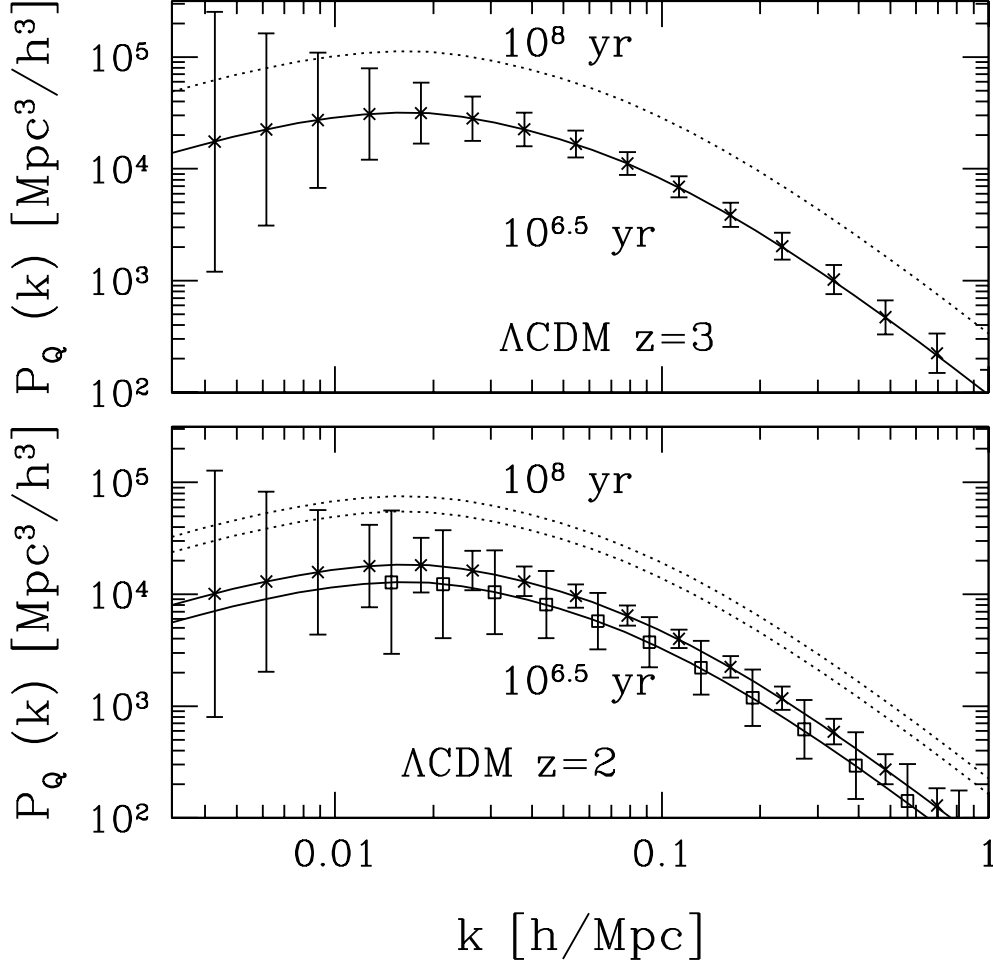


FIG. 4.— Three-dimensional power spectrum  $P_Q(k)$  of quasars in  $\Lambda\text{CDM}$  at two different redshifts near the peak of the comoving quasar abundance. Results are shown for quasars with  $B \leq 20.4$  (or  $g' \lesssim 19$ ), in the long (dotted curves) and short lifetime (solid curves) models, together with the expected  $1\sigma$  error bars from SDSS (crosses) with an assumed area of  $\pi$  steradians. The slightly lower curves in the lower panel refer to 2dF (open squares), with a magnitude cut of  $B = 20.5$ , and show the expected error bars from an assumed area of 0.23 steradians.

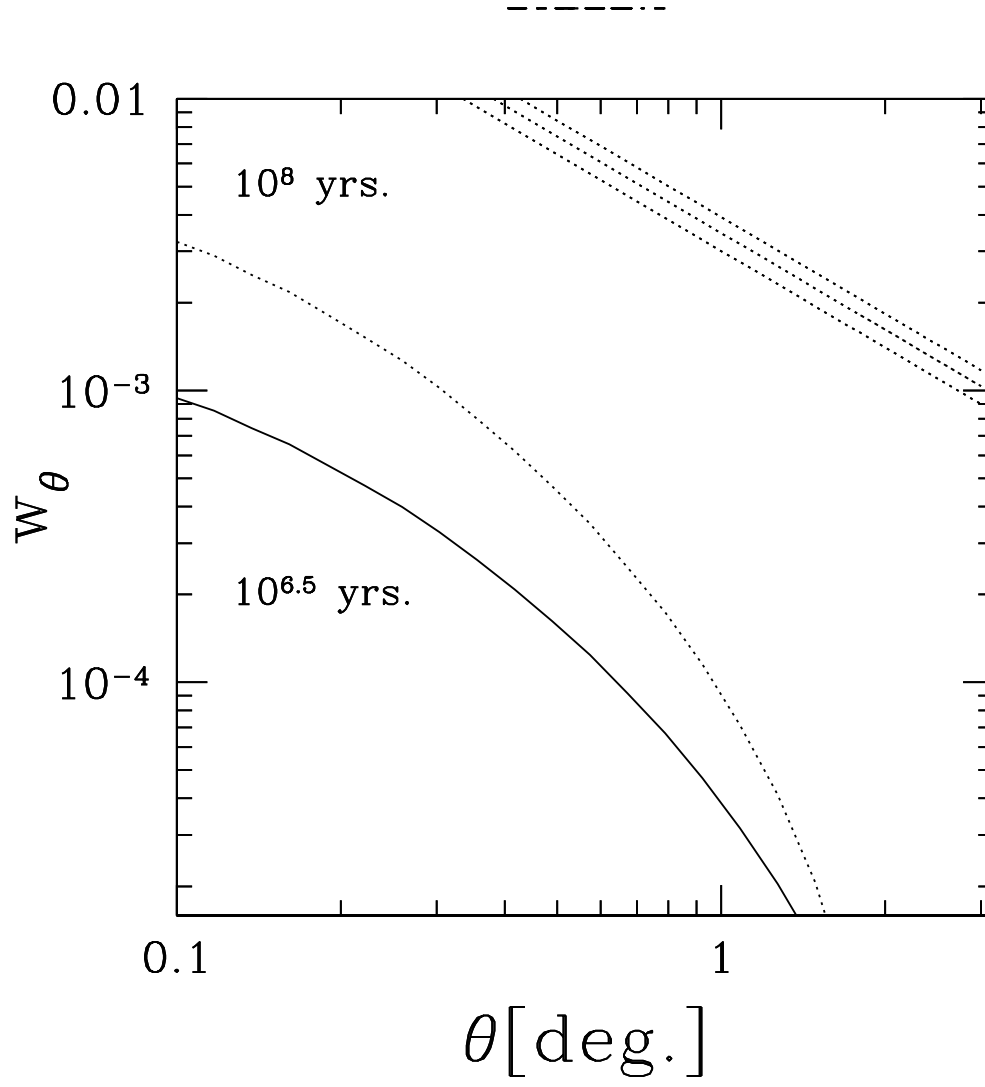


FIG. 5.— Angular correlation function of the total XRB,  $w_\theta$  at  $E = 1$  keV. The dashed lines in the upper right corner indicate  $w_\theta$  at  $E = 1.15$  keV with quoted  $\pm 1\sigma$  uncertainties as measured from the ROSAT All Sky Survey (Soltan et al. 1999), which can be considered an upper limit.

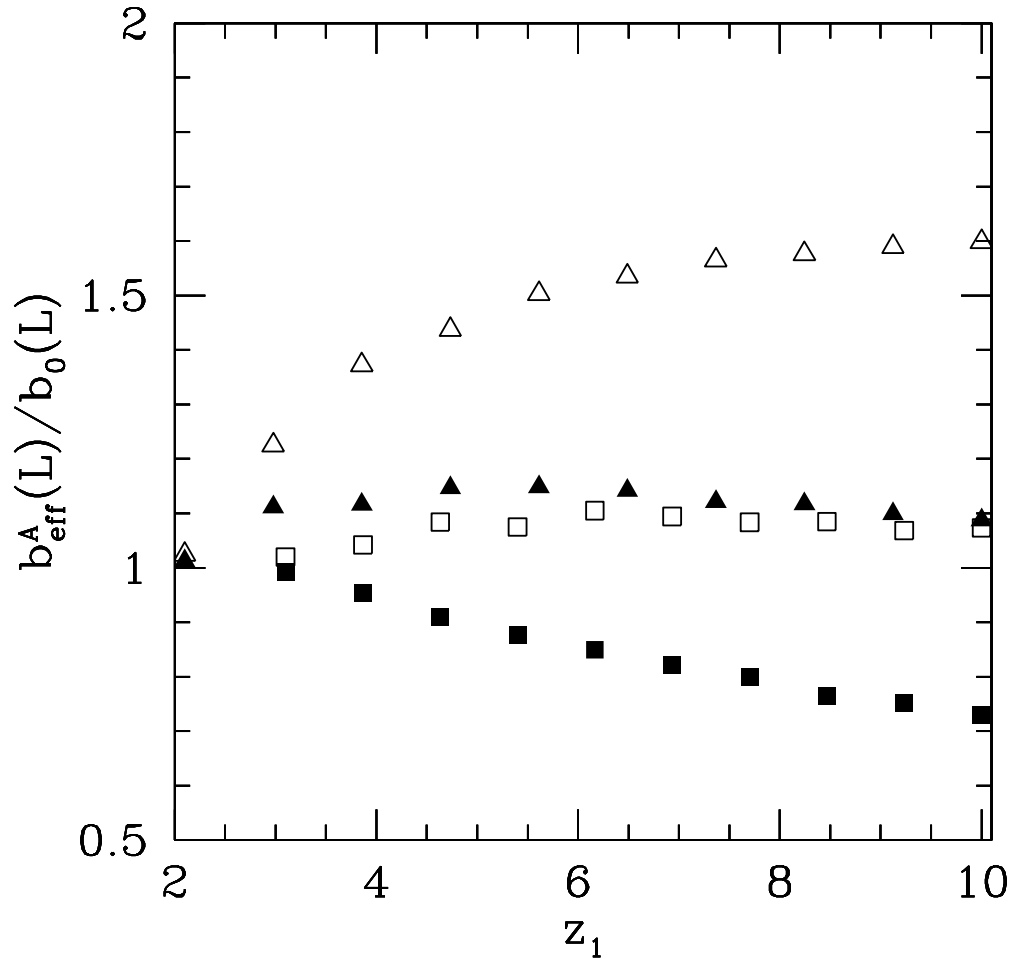


FIG. 6.— The ratio of the effective bias  $b_{\text{eff}}^A(L)$  (in a model allowing multiple quasars per halo) to the original bias  $b_0(L)$  (for one quasar per halo) as a function of  $z_1$  at fixed luminosity  $L$ , where  $z_1$  is the redshift when sub-halos are identified. The squares (open for  $M_0 = 10^{12.5} M_\odot$  and solid for  $M_0 = 10^{13.5} M_\odot$ ) show this relation for quasars at  $z_0 = 3$ , whereas the triangles are for  $z_0 = 2$  (open for  $M_0 = 10^{12} M_\odot$  and solid for  $M_0 = 10^{13} M_\odot$ ). The model is  $\Lambda$ CDM. See text for discussions.



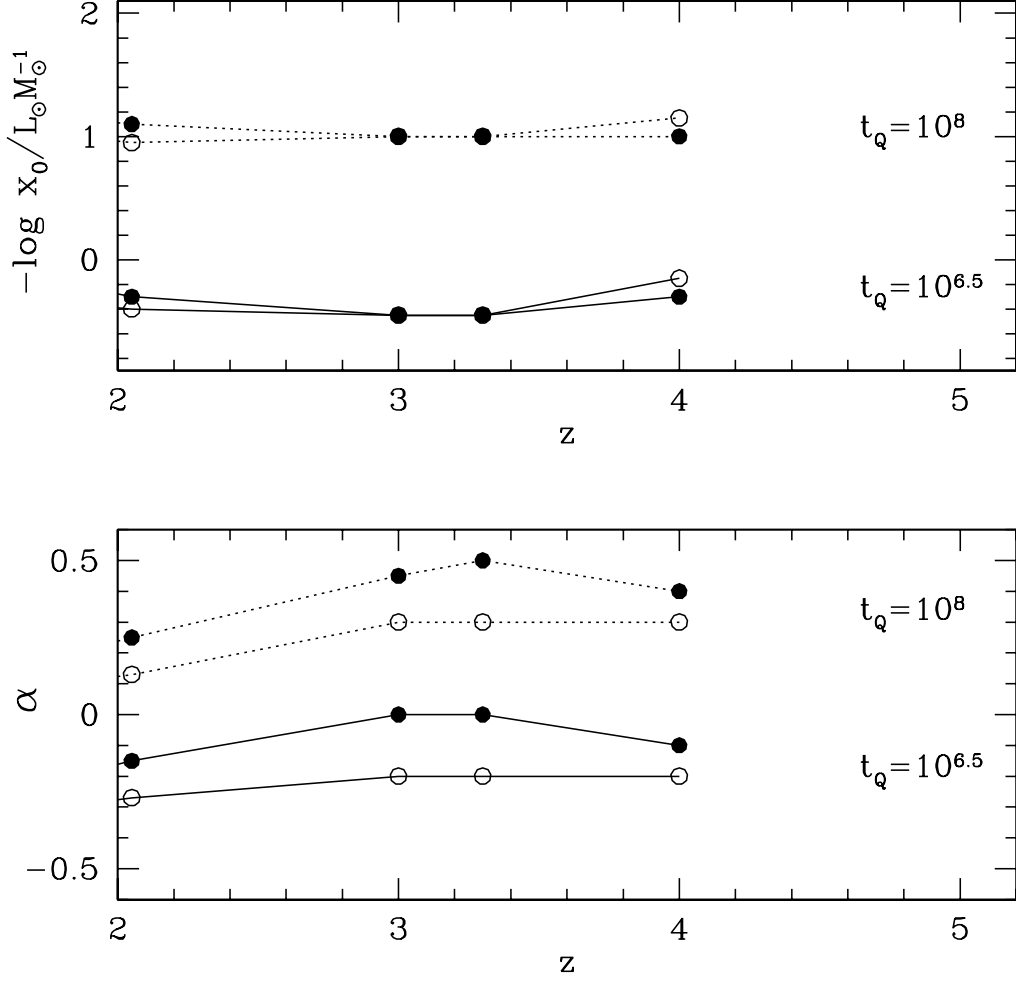


FIG. 7.— Fitting parameters  $\alpha(z)$  and  $x_0(z)$  for the mean relation between B-band quasar luminosity  $L_B$  and halo mass  $M_{\text{halo}}$  given in equation 20, for two different quasar lifetimes  $t_Q = 10^{6.5}$  (solid curves) and  $t_Q = 10^8$  yr (dotted curves). The filled dots correspond to a  $\Lambda$ CDM and the open dots to an OCDM cosmology. In all cases, we assumed a scatter with  $\sigma = 0.5$  (cf. eq. 16) around the mean  $L - M_{\text{halo}}$  relation.

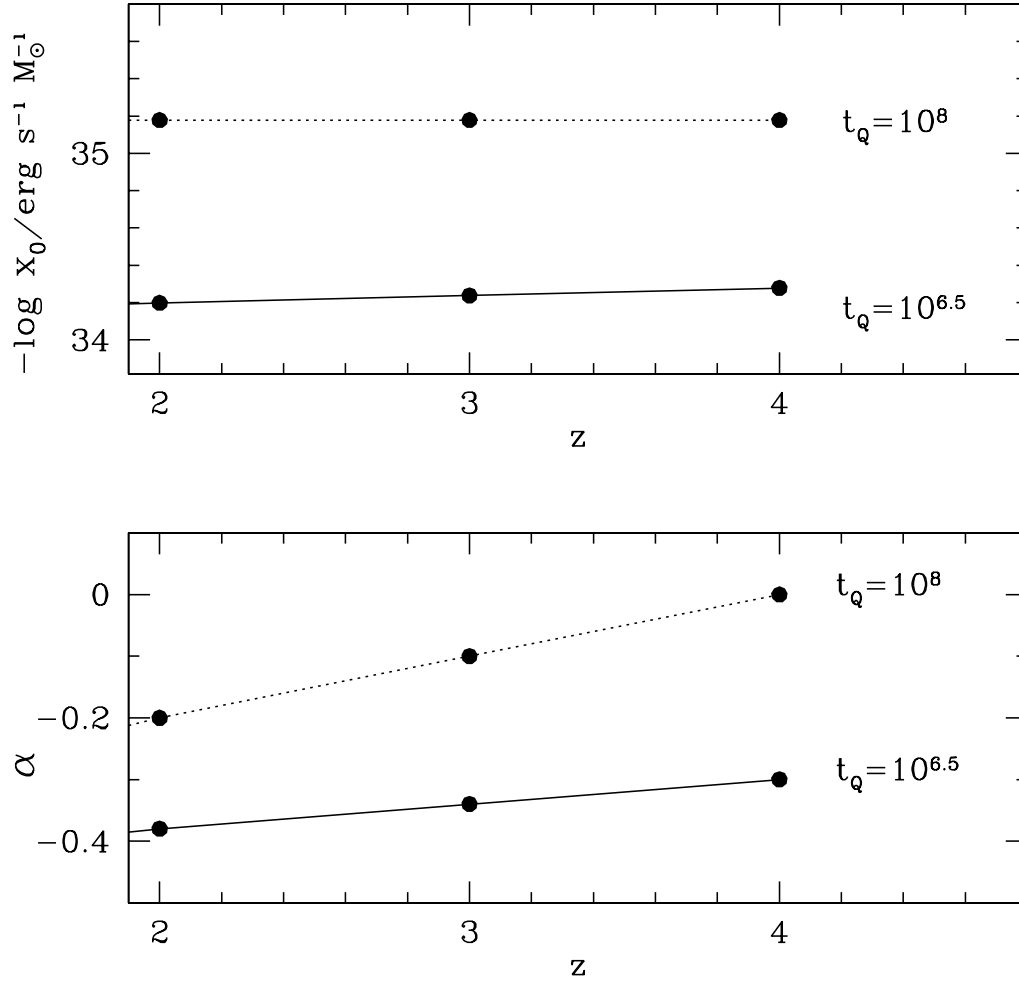


FIG. 8.— Same as Figure 7, except the X-ray quasar luminosity is used at 1keV. Only the  $\Lambda$ CDM case is shown.